Structure and Properties of Sn(II)–β″-Alumina

G. S. Rohrer,* J. O. Thomas,† and G. C. Farrington

Department of Materials Science and Engineering, University of Pennsylvania, 3231 Walnut St., Philadelphia, Pennsylvania 19104

Received February 7, 1990

Single crystals of Sn(II)–β″-alumina, synthesized by ion exchange from the fast ion conductor Na–β″-alumina, have been found to react with water vapor to form a hydrated compound with the formula $Sn_{0.83}Mg_{0.67}Al_{10.33}O_{17}\cdot(H_2O)_x$. Thermogravimetric analysis, evolved gas analysis, and differential scanning calorimetry have been used to determine that x can vary between 0.0 and 0.74 and that the binding energy of the water is 0.75 eV. The anhydrous compound is luminescent under UV excitation. Luminescence spectra show a broad band in the visible range which can be assigned to the $^3P_1$ to $^1S_0$ transition. Ac impedance spectroscopy has been used to determine that the ionic conductivity of the anhydrous compound is 1.5×10^{-2} $(\Omega\cdot cm)^{-1}$ at 500 °C and 1.5×10^{-5} $(\Omega\cdot cm)^{-1}$ at 70 °C. Single-crystal X-ray diffraction studies were performed on both an anhydrous crystal and a hydrated crystal with $x = 0.74$. The crystals are in the rhombohedral space group, $R\bar{3}m$, and there are three formula units per unit cell. The hexagonal cell dimensions for the anhydrous compound are $a = 5.6206$ (5) Å, $c = 34.311$ (7) Å, $V = 936.8$ (3) Å^3, and the dimensions for hydrated compound are $a = 5.623$ (1) Å, $c = 34.191$ (11) Å, $V = 930.5$ (4) Å^3. The structure is strongly influenced by the lone pair on the Sn(II) ion. The effect of intercalated water on the structure and physical properties is discussed.

Introduction

Na(I)–β″-alumina is a high-conductivity solid electrolyte for sodium ions with the general formula $Na_{1+x}Mg_xAl_{11-x}O_{17}$, $x \approx 0.67$. The high ionic but low electronic conductivity of Na(I)–β″-alumina has made it a promising solid electrolyte for use in batteries and electrochemical devices, and thus a great deal of research has been devoted to the development of high-conductivity polycrystalline ceramics for these applications. It is also possible to exchange the Na(I) in Na(I)–β″-alumina for a wide variety of mono-, di-, and trivalent cations. For example, complete or partial exchange occurs with at least 8 monovalent, 11 divalent, and 9 trivalent cations.[1,2] This remarkable ion-exchange chemistry has produced many new and unusual compounds, most of which cannot be synthesized directly. Some have been shown to have possible applications as solid electrolytes[3] and solid-state lasers.[4]

Although many divalent β″-aluminas have been synthesized and characterized, little work has appeared on Sn(II)–β″-alumina, a composition particularly interesting because of the "lone-pair" character of the Sn(II) ion. Hellstrom and Benner[5] have reported the synthesis of polycrystalline Sn(II)–β″-alumina ceramics that were described as discolored and mechanically weak, and Sattar et al.[2] reported the synthesis of partially exchanged Sn(II)–Na(I)–β″-alumina crystals that were described as "severely cracked". In this paper we report the synthesis of intact, fully exchanged single crystals of Sn(II)–β″-alumina, $Sn_{0.83}Mg_{0.67}Al_{10.33}O_{17}$. In addition, we have characterized these samples with respect to their composition, ionic conductivity, optical absorption, luminescence, and crystal structure.

Na(I)–β″-alumina is a layered solid electrolyte that consists of close-packed Al_2O_3 layers, each 11 Å thick, separated by loosely packed conduction layers. Mobile sodium ions and sodium ion vacancies are located in the conduction layers, and the Mg(II) ions are substituted on Al(III) sites in the Al_2O_3 layers, which are referred to as spinel blocks. The framework is essentially the same in each isomorph, but the arrangement of mobile cations in the conduction layers varies considerably.[6] In general, the arrangement of the mobile cations and vacancies is influenced both by interactions between the mobile ions and the framework and by interactions among the mobile ions themselves.

The structure and properties of Sn(II)–β″-alumina are particularly interesting because the $5s^2$ electronic configuration of its outer shell makes Sn(II) a "lone-pair" ion. Repulsion between the nonbonding lone-pair electrons and nearby ligands usually results in an asymmetric ligand arrangement (the "lone-pair effect"). The substitution of Sn(II) for Na(I) in the β″-alumina structure could be expected to produce an interesting example of the lone-pair effect. In other compounds, Sn(II) ions are introduced as the entire structure is formed, so that the lone-pair distortions can be accommodated by the surrounding anions. However, in Sn(II)–β″-alumina, the Sn(II) ions are introduced into an already existing framework. The mobile ions usually occupy nearly symmetric sites surrounded by oxygen ions. The two most common are the tetrahedral Beevers–Ross (BR) and the roughly octahedral midoxygen (mO) sites. If the repulsion between the lone pair on Sn(II) and the oxygens is large enough, we would expect the cation to distort these normally symmetric sites.

Another source of interest in Sn(II)–β″-alumina was the possibility that its ionic conductivity might be unusually high, similar to that of Pb(II)–β″-alumina. The ionic conductivity of Pb(II)–β″-alumina is much higher than the other divalent isomorphs, which all have similar conductivities.[7] Although the reason for this is not clear, the high electronic polarizability of the Pb(II) ion has been proposed as one possible explanation. Since Pb(II), like Sn(II), is a lone-pair ion, one motivation for this investigation was to determine whether the chemical similarity of these two

† Institute of Chemistry, University of Uppsala, Box 531, S-751 21 Uppsala, Sweden.

(1) Farrington, G. C.; Briant, J. *Fast Ion Transport in Solids*; Vahista, P., Mundy, J. N., Shenoy, G. K., Eds.; North Holland: Amsterdam, 1977; p 395.
(2) Sattar, S.; Ghosal, B.; Underwood, M. L.; Mertwoy, H.; Saltzberg, M. A.; Frydrych, W. S.; Rohrer, G. S.; Farrington, G. C. *J. Solid State Chem.* **1986**, *65*, 231.
(3) Cole, T. *Science* **1983**, *221*, 915.
(4) Farrington, G. C.; Dunn, B.; Thomas, J. O. *Cryst. Lattice Defects Amorph. Mater.* **1985**, *12*, 497.
(5) Hellstrom, E. E.; Benner, R. E. *Solid State Ionics* **1983**, *11*, 125.
(6) Thomas, J. O.; Alden, M.; Farrington, G. C. *Solid State Ionics* **1983**, *9*, 301, and references therein. Also: Farrington, G. C.; Dunn, B.; Thomas, J. O. The Multivalent β″-Aluminas, in press.
(7) Seevers, R.; DeNuzzio, J.; Farrington, G. C.; Dunn, B. *J. Solid State Chem.* **1983**, *50*, 146.

0897-4756/90/2802-0395$02.50/0

ions might mean that Sn(II)-β''-alumina is also highly conductive.

We also examined the hydration reactions of Sn(II)-β''-alumina, since it has been known for some time that the properties of several β''-alumina isomorphs are water sensitive. The hydration reactions of monovalent β''-aluminas are already well-known.[8] Recent results have shown that Ca(II)-, Ba(II)-, Pb(II)-, and Sn(II)-β''-alumina react readily with water vapor to form hydrated compounds,[9] yet no study of the structures of the hydrated divalent compounds has been reported. The work described in this paper has thus focused in part on understanding the effect of water on the structure and properties of Sn(II)-β''-alumina. We have measured the extent of the hydration reaction in Sn(II)-β''-alumina, the stability of the hydrated material, and the enthalpy of the dehydration reaction. We have also shown that the penetration of water into the conduction planes alters the mobile ion distribution and the optical properties of the compound.

Finally, β''-alumina's nearly universal acceptance of cations makes it a versatile optical host material, and thus some of the most interesting new applications proposed for β''-alumina isomorphs have been as phosphors[10] and solid-state laser materials.[11] Our characterization of the optical properties of Sn(II)-β''-alumina, described in this paper, has shown that it is strongly luminescent in the visible range.

Experimental Procedures

Synthesis of Sn(II)-β''-Alumina. Single crystals of Na-β''-alumina were grown by the flux evaporation method described previously.[12] The crystals were then doped with ^{22}Na, a radioactive tracer used to determine the extent of subsequent ion exchange. After determination of the weight and ^{22}Na activity of each crystal, samples were immersed in molten anhydrous $SnCl_2$ at 400 °C. The molten exchange salt was contained in an alumina boat, and the reactions were performed in a dry, inert atmosphere. Generally, two reactions in fresh salt, each of about 20-min duration, produced crystals that were fully exchanged, as indicated by weight change and the decrease of the ^{22}Na activity to zero.

In addition, a partially exchanged sample was prepared in the following way. A rectangular crystal of Na(I)-β''-alumina was immersed in molten $SnCl_2$ in air for 10 s at 300 °C. After being cleaned, the sample was annealed at 600 °C for 5 h to homogenize the Sn(II) distribution. Before annealing, luminescence was observed only around the edges of the crystal. However, after annealing, the luminescence was uniform. By measuring the decrease in the ^{22}Na activity, it was determined that 7% of the sodium had been replaced by Sn(II) to create a composition $Na_{1.55}Sn_{0.06}Mg_{0.67}Al_{10.33}O_{17}$.

Other partially exchanged crystals were prepared for optical absorption measurements by equilibrating single crystals in molten $SnCl_2/NaNO_3$ mixtures at 400 °C. Exchange salt compositions varied from 0.1 to 5 mol % Sn(II). The compositions of the crystals were not determined. The object here was only to produce samples with low but different doping levels of Sn(II).

Immediately following ion exchange, the crystals had a slightly yellow tinge. The color was nonuniform, being more intense at edges and cracks and disappeared after annealing briefly in air at 600 °C. This was presumably because salt from the exchange bath had become trapped in cracks and cleavage planes and was easily volatilized during the high temperature annealing. We have observed this same phenomenon with other ion-exchange reactions.

Although most samples developed some cracks during the ion-exchange process, others remained intact and suitable for single-crystal ionic conductivity measurements. These were cut into rectangular platelets, and electrodes applied to the appropriate faces. Other single-crystal samples were crushed with an alumina mortar and pestle and sieved to 40–150-μm powders for TGA and DSC measurements.

Thermogravimetry, Differential Scanning Calorimetry, and Evolved Gas Analysis. The apparatus used for the thermal analysis experiments has been described previously,[13] and the methods used are described below. First, each crushed sample was heated at 425–450 °C in the thermogravimetry (TG) cell until a constant "dry" weight was attained. The sample was then cooled to room temperature at 0.5 °C/min in a flowing wet gas, during which a typical weight gain was 2%. Portions of the samples were then decomposed by heating in the TG-EGA cell at 10 °C/min in a flowing inert atmosphere so that the evolved gas could be analyzed. Other portions were decomposed in the DSC cell at 10 °C/min in nitrogen gas to measure the enthalpy of dehydration.

Ionic Conductivity. Ac impedance spectroscopy was used to measure the ionic conductivity of a single crystal of Sn(II)-β''-alumina. A small crack-free single-crystal was cut into a rectangular slab of dimensions 0.195 × 0.215 × 0.025 cm. Gold blocking electrodes were applied to two faces of the crystal perpendicular to the conduction planes. Silver paint was applied on top of the gold to ensure good contact with the platinum electrodes of the spring-loaded conductivity cell. During the entire measurement, 99.999% pure, dried argon was flowed through the cell. Impedance measurements were made at 18 temperatures between 500 and 50 °C in the frequency range 100 Hz to 13 MHz using a previously described automated temperature control and impedance measurement system.[13] The same measurement was performed on the partially exchanged sample for comparison.

Optical Absorption and Luminescence. Optical absorption measurements were made with a Perkin-Elmer Lambda 4C spectrophotometer. Emission and excitation spectra were measured with a Perkin-Elmer MPF-66 spectrophotometer. Low-temperature spectra were obtained by using an Oxford Instruments liquid nitrogen cryostat. In all cases, single-crystal platelets were used for the measurements.

Single-Crystal X-ray Diffraction. Single-crystal X-ray diffraction studies were performed on both an anhydrous crystal and a hydrated crystal. The hydrated crystal was selected from the crushed sample that was prepared in the TGA. The anhydrous crystal was treated at 600 °C in air. TGA experiments indicated that this treatment prevents any subsequent water absorption on cooling. This point will be discussed further in the Results and Discussion.

The diffraction measurements were performed on a Nonius CAD4 automatic four-circle X-ray diffractometer using graphite-monochromatized Mo Kα radiation. Preliminary studies of each crystal confirmed that the $R\bar{3}m$ space group of Na-β''-alumina was retained in these samples. Reflections were collected out to sin $\theta/\lambda = 0.905$ Å^{-1}. The data were corrected for background, Lp effects, and absorption. The absorption correction was made using calculated absorption coefficients (26.1 cm^{-1} for

Table I. Some Details of the Diffraction Experiment and the Refinements

	anhydrous	hydrated
abs coeff μ, cm^{-1}	26.1	26.5
transmission factor	0.82 and 0.58	0.85–0.82
sin θ/λ_{max}, Å^{-1}	0.951	0.905
no. of indep reflns	1781	1553
R factor for monitor reflns	0.011	0.008
R factor for refinement of F_o^2	0.072	0.062
R factor for refinement on F_o	0.046	0.040
no. of reflns used ($>2\sigma(F^2)$)	1503	1100
unit cell dimension a, Å	5.6206 (5)	5.623 (1)
unit cell dimension c, Å	34.311 (7)	34.191 (11)
cell vol, Å^3	936.8 (3)	930.5 (4)

(8) Garbarczyk, J.; Jakubowski, W.; Wasiucionek, M. *Solid State Ionics* **1983**, *9*, 249. Bates, J. B.; Wang, J. C.; Dudney, N. J.; Brundage, W. E. *Solid State Ionics* **1983**, *9*, 237. Dudney, N. J.; Bates, J. B. *J. Am. Ceram. Soc.* **1987**, *70*, 816.

(9) Rohrer, G. S.; Farrington, G. C. *Mater. Res. Bull.* **1988**, *23*, 1747.

(10) Ghosal, B.; Mangle, E. A.; Topp, M. R.; Dunn, B.; Farrington, G. C. *Solid State Ionics* **1983**, *9*, 273.

(11) Dunn, B.; Yang, D. L.; Vivien, D. *J. Solid State Chem.* **1988**, *73*, 235.

(12) DeNuzzio, J. Ph.D. Thesis, University of Pennsylvania, 1986.

(13) Rohrer, G. S.; Farrington, G. C. *Chem. Mater.* **1989**, *1*, 438.

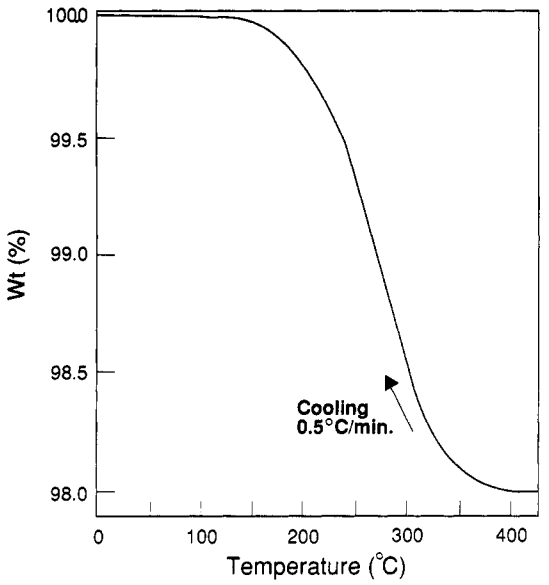

Figure 1. Thermogram showing the hydration of Sn(II)-β″-alumina. The sample was cooled at 0.5 °C/min in flowing humid N_2.

the anhydrous and 26.5 cm^{-1} for the hydrated crystal) and an explicit description of the crystal's morphology. The transmission factor for different reflections varied between 0.58 and 0.82 for the anhydrous crystal and between 0.82 and 0.85 for the hydrated crystal. A number of reflections suspected to be affected by multiple reflection were eliminated from the data set for the hydrated crystal. Details of the diffraction experiments are summarized in Table I. The refinement was based on minimizing the function $\sum w(F_o^2 - |F_c|^2)^2$, where the weighting function, w, is of the form $w = 1/\sigma^2(F_o^2)$, and $\sigma^2(F_o^2) = \sigma_{count}^2(F_o^2) + (kF_o^2)^2$, and k is an empirical constant set to 0.04. Reflections with $F_o^2 < 2\sigma(F_o^2)$ were not used in the refinements.

Results and Discussion

Synthesis. Ion exchange of Sn(II) for Na(I) proceeds rapidly at 400 °C. The single crystals used were several millimeters in diameter, yet ion exchange was complete after only 40 min. We found that both higher temperatures and longer exposures to the exchange salt increased the tendency for cracking. Exposure at 400 °C for 40 min produced fully exchanged samples, some of which were free from cracks. The Sn(II)-β″-alumina samples were much more brittle than samples of Na(I)-β″-alumina. Diffraction measurements show that the c-lattice parameter increases from 33.54 Å in the Na(I) form[5] to 34.311 (7) Å in the Sn(II) form. Sn(II)-β″-alumina has the second-largest c parameter of any known isomorph of β″-alumina, exceeded only by ammonium/hydronium-β″-alumina.[14] Such a lattice dilation suggests that the crystals are subjected to compressive stresses, which may be the reason many crystals crack. Similar effects have been observed as the result of ion exchange with very small ions such as Mg(II) and Li(I), in which cracking is the result of tensile stresses.[15]

To determine the extent of ion exchange, we monitored both the elimination of ^{22}Na from the crystal, which indicates that all of the mobile Na(I) has been replaced, and the weight change, which provides information as to how its charge has been compensated for. In this case, a 9.1% weight increase was observed for samples in which the amount of radiotracer was reduced to an undetectable level; precisely the weight change expected for complete replacement of Na(I) by Sn(II). Complementary measurements are especially important with ions such as Sn(II), which can assume more than one valence state.

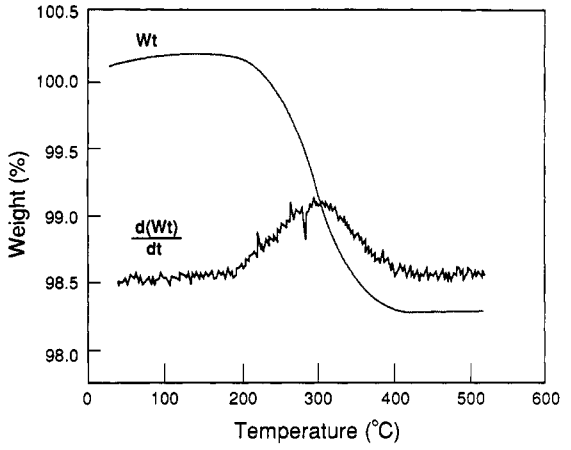

Figure 2. Thermogram showing the dehydration of Sn(II)-β″-alumina. The sample was heated at 10 °C/min in flowing dry N_2.

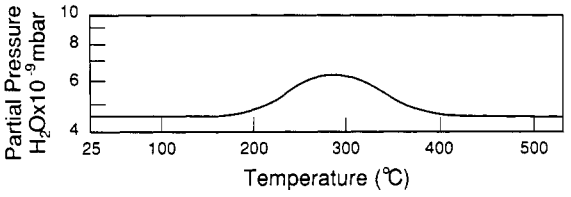

Figure 3. Thermogram showing the partial pressure of H_2O over Sn(II)-β″-alumina during the dehydration reaction. This thermogram was recorded simultaneously with that shown in Figure 2.

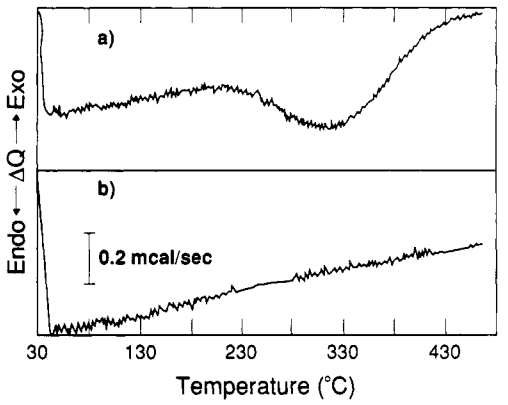

Figure 4. Differential scanning calorimetry trace for Sn(II)-β″-alumina heated at 10 °C/min in dry N_2. Figure 4a shows the trace from the initial heating following the synthesis (see Figure 1). Figure 4b shows the repeat run following a quench from 500 °C.

Thermal Analysis. We used a variety of thermal analysis techniques to study the reactivity of Sn(II)-β″-alumina with water. The thermogram for the hydration of Sn(II)-β″-alumina is shown in Figure 1. The sample increased in weight upon cooling from about 350 to 100 °C. The total weight gain was 2.0% of the dry weight, which indicates that the final composition was $Sn^{II}_{0.33}Mg_{0.67}Al_{10.33}O_{17}\cdot(H_2O)_{0.74}$. Figure 2 shows the thermogram for the dehydration reaction. A 2.0% weight loss occurred between 200 and 400 °C. The mass spectrometer measured an increase (Figure 3) in the partial pressure of water vapor over the sample simultaneous with the weight loss. The partial pressures of the other four gases monitored during the experiment remained constant throughout.

(14) Thomas, J. O.; Farrington, G. C. *Acta Crystallogr.* **1983**, *B39*, 227.
(15) Farrington, G. C.; Dunn, B. *Solid State Ionics* **1982**, *7*, 267.

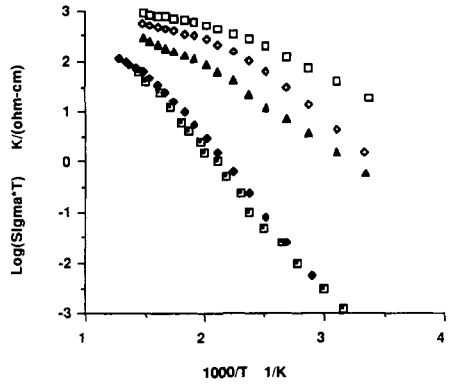

Figure 5. Arrhenius plot for the ionic conductivity of Sn(II)–β″-alumina (filled diamonds). The high-temperature activation energy is 0.25 eV, and the low-temperature activation energy is 0.59 eV. The conductivities of several other isomorphs are included for comparison. Open squares, Na(I)–β″-alumina; open diamonds, 7% Sn(II)-doped Na(I)–β″-alumina; triangles, Pb(II)–β″-alumina; filled diamonds, Sn(II)–β″-alumina; filled squares, Ba(II)–β″-alumina.

From this, we have concluded that the increase in weight during cooling in wet gas and the subsequent weight loss on heating in dry gas were the result of the intercalation and deintercalation, respectively, of water.

Figure 4a shows the DSC trace for the dehydration reaction of Sn(II)–β″-alumina at a heating rate of 10 °C/min in dry nitrogen gas. During heating, an endothermic transition was observed to occur in the same temperature range as the weight loss and increase in water vapor pressure previously discussed. After heating, the sample was removed from the cell and quenched to room temperature, and the experiment repeated. This time, however, no endotherm was observed (see Figure 4b). The endotherm visible in the first experiment was presumably due to the evolution of water from the sample; it was absent from the second run because the water had already been removed.

The calorimetry data were used to calculate that the dehydration energy is 0.75 eV per water molecule, which is comparable to values reported for other divalent β″-alumina isomorphs.[9] The similarity of the dehydration energies suggests that water occupies similar crystallographic sites in each isomorph and that the dominant interaction of water molecules in β″-alumina is with the framework rather than with the mobile ions. This will be discussed further in relation to the structural results.

We also found that a sample that had previously been heated above 500 °C in air loses its ability to absorb water but regains it after heating in wet nitrogen gas in the same temperature range. We believe that heating in air passivates the surface of the sample through a reversible reaction. This effect is normally avoided by working in nitrogen gas but was exploited in this work to protect selected samples from unwanted hydration during structural and optical experiments.

Ionic Conductivity. The Arrhenius-type plot for the ionic conductivity of Sn(II)–β″-alumina is shown in Figure 5; conductivity plots for one partially exchanged sample as well as several other isomorphs are included for comparison. The chemical similarity of Sn(II) and Pb(II) ions suggested that Sn(II)–β″-alumina might exhibit the same anomalously high conductivity as Pb(II)–β″-alumina. However, the conductivity of Sn(II)–β″-alumina was found to be comparable to that of other divalent β″-aluminas such as the Ca(II), Ba(II), Eu(II), Cd(II), and Sr(II) forms, all of which have conductivities much lower than that of Pb(II)–β″-alumina at moderate temperatures.[16] The structural data presented later in this section indicate that Sn(II) interacts strongly with the host lattice and is localized in the tetrahedral BR site at room temperature. In comparison, structural data for the Pb(II) isomorph indicate that Pb(II) ions occupy lower symmetry sites displaced from the 3*m* axis.[6] These observations are consistent with the observed differences in the ionic conductivities. Simply stated, greater localization of the cations leads to lower ionic conductivity.

The conductivity of the 7% exchanged sample is intermediate between those of the pure Na(I) form and pure Sn(II) forms. as Na(I) is replaced by Sn(II), several factors affecting ionic conductivity change. First, the concentration of relatively mobile Na(I) ions decreases, and the concentration of less mobile Sn(II) ions increases. This should decrease the ionic conductivity. On the other hand, as divalent cations are added, the vacancy concentration increases, since two Na(I) ions are replaced by one Sn(II) ion and a vacancy. In the absence of other effects, increasing the vacancy concentration should increase the ionic conductivity. Since the introduction of a small amount of Sn(II) results in a substantial decrease in ionic conductivity, the first effect would appear to take precedence over the second.

There is a definite change in the slope of the Arrhenius-type plot of the ionic conductivity of Sn(II)–β″-alumina. The activation energy shifts from 0.59 eV below about 375 °C to 0.25 eV above. The conductivity of the partially exchanged sample also shows a distinct change in activation energy, from 0.39 eV at low temperature to 0.10 eV at higher temperature. It has been suggested that changes in the activation energy for ionic conduction in the β″-alumina system can be attributed to ordering processes among the mobile cations and vacancies.[17] In this case, no direct crystallographic evidence for an ordered superlattice at room temperature has been found.

It might also be suggested that this increase in activation energy results from hydration of the crystal during the cooling cycle of the conductivity measurement. We carried out several experiments to test this hypothesis. First, it was found that single crystals of Sn(II)–β″-alumina absorb water extremely slowly from the dried gas used in the measurement, presumably because of their small surface-to-bulk ratio and the low partial pressure of water in the gas. In addition, the room-temperature conductivity of a crystal measured at the end of the extended heating and cooling cycle used in the normal conductivity experiments was the same as after the sample had been heated to 500 °C and then quenched to room temperature. Thermal analysis measurements show that even powders do not absorb measurable amounts of water when quenched rapidly from a temperature above the dehydration temperature. From these observations, it would appear that hydration is not the cause of the change in the activation energy. The true cause may be an abrupt change in the arrangement of the cations in the conduction layer, a possibility that will be explored in future work by molecular dynamics simulation studies and high-temperature diffraction experiments.

Optical Absorption and Luminescence. The ultraviolet absorption of Sn(II)–β″-alumina was so strong that a useful absorption spectrum could not be obtained on fully exchanged samples. However, partially exchanged samples were examined at room temperature, and two bands were observed to grow as the Sn(II) concentration

(16) Dunn, B.; Ostrom, R. M.; Seevers, R.; Farrington, G. C. *Solid State Ionics* **1981**, *5*, 203. Also, refs 7 and 10.
(17) Sato, H.; Kikuchi, R. *J. Chem. Phys.* **1971**, *55*, 677.

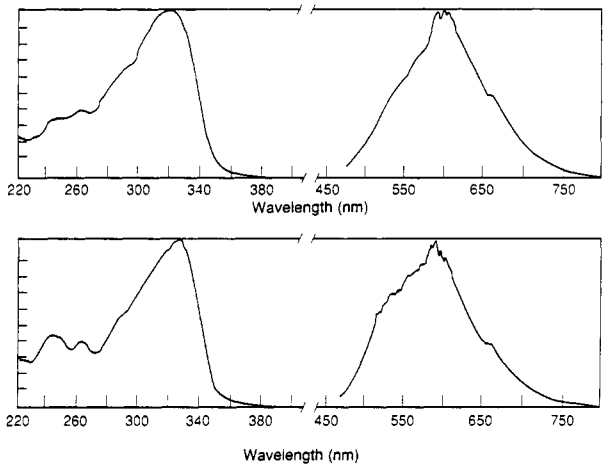

Figure 6. Excitation and emission spectra for Sn(II)-β″-alumina at liquid nitrogen temperature. In the upper graph, the excitation spectrum was obtained from the emission at 601 nm. The emission spectrum was obtained by using an excitation at 323 nm. In the lower graph, the excitation spectrum was obtained from the emission at 538 nm. The emission spectrum was obtained by using an excitation at 243 nm.

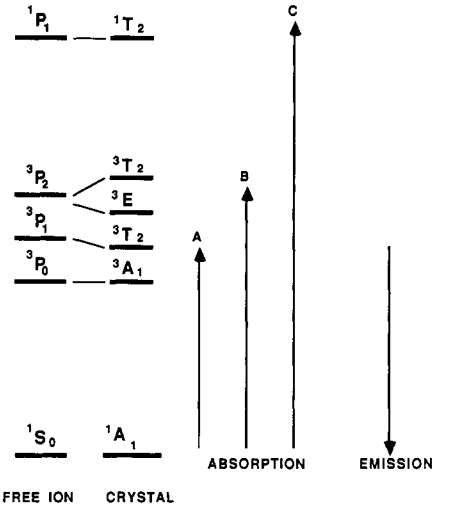

Figure 7. Energy level diagram for Sn(II) in a tetrahedral environment.

increased. A very strong broad band was observed centered at 250 nm and an additional weaker band at 335 nm. The intensity ratio of the two bands is approximately 8:1. The samples also displayed a very strong orange emission when illuminated with an ultraviolet lamp. Excitation spectra of fully exchanged samples revealed excitation bands that coincide with the bands observed in the absorption experiment. Figure 6 shows excitation and emission scans recorded at liquid nitrogen temperature. These excitation spectra show additional structure not observed in the room-temperature absorption spectra.

The optical properties of the Sn(II) ion in octahedral coordination are well-known.[18] The diffraction measurements discussed later in this section indicate that the Sn(II) ions are tetrahedrally coordinated in the β″-alumina framework. This different symmetry affects the splitting of the $^3P_2$ state. However, transitions to this state from the $^1S_0$ ground state are forbidden and not observed in most materials. Aside from this alteration, one would expect the order, but not necessarily the spacing, of the other energy levels to remain the same. The transitions observed in absorption and excitation are of the type $5s^2$ to $5s^15p^1$. We have assigned the two observed bands in the following way: the weak low-energy band at 335 nm is the $^1S_0$ to $^3P_1$ band ($^1A_1$ to $^3T_2$), commonly referred to as the A band; the strong higher energy band at 253 nm is the $^1S_0$ to $^1P_1$ band ($^1A_1$ to $^1T_2$), usually referred to as the C band. The emission band is due to the $^3P_1$ to $^1S_0$ ($^3T_2$ to $^1A_1$) transition.

The A and C bands are typically observed in materials containing Sn(II). A higher energy D band corresponding to a perturbed exciton is sometimes also observed.[19] In our case, only two bands were resolved in the absorption spectrum. Their energies are comparable to the C and A band energies found for Sn(II) impurities in KBr and KI.[18] Also, the C band transition is fully allowed, while the A band is partially forbidden and made allowed only by spin–orbit mixing. As a result, the observed C to A band intensity ratio is 10:1 for Sn(II) in alkali-metal halides. We have observed an intensity ratio of approximately 8:1 in Sn(II)-β″-alumina. Both the position and intensities of the observed bands support the assignment. It should also be mentioned that the structure of the excitation spectrum at 77 K agrees qualitatively with that predicted for the Sn(II) ion in a tetrahedral environment.[20] The excitation spectra indicate that the majority of the emitted light comes from the A excitation rather than the fully allowed C excitation. We have therefore assigned the emission band as the $^3P_1$ to $^1S_0$ ($^3T_2$ to $^1A_1$) transition. This is the same transition assigned to the emission band in Sn(II) doped alkali-metal halide phosphors.[19] A simple energy level diagram is shown in Figure 7.

The emission spectra show a broad band with two closely overlapping sections in the visible region. The high-energy part is preferentially excited by the high-energy absorption band (see Figure 6). A similar effect has been observed for Sn(II) in alkali-metal halides,[19] where the splitting in both the emission and absorption bands has been attributed to the Jahn–Teller effect. In our case, the split emission band may also arise from the emission of ions in different environments. Because the BR sites are only partially occupied by Sn(II), each Sn(II) ion will have 0, 1, 2, or 3 other Sn(II) ions at adjacent BR sites. A more detailed spectroscopic study would be required to establish which of these models applies.

Regardless of the reason for the split emission band, its primary source is excitation in the A band. This band is completely quenched by hydration. This same reduction in fluorescent intensity has been noted for the Eu(II)[21] and Nd(III)[22] isomorphs. In addition, hydration converts the sample from a colorless to a yellow powder. This color change and the loss of luminescence are reversible by dehydration. It is clear that hydration has a dramatic effect on the optical properties of these materials. The prevention of hydration will surely be an important factor in the design of any optical devices incorporating them.

Structure Analysis. The structures of both anhydrous and hydrated Sn(II)-β″-alumina have been studied. They comprise essentially two parts: the aluminum oxide "framework" and the conduction layers in which the mobile cations and water molecules reside. With the exception of some characteristic distortions, the framework of Na(I)-β″-alumina is retained during ion exchange. It consists

(18) McClure, D. S. *Electronic Spectra of Molecules and Ions in Crystals*; Academic Press: New York, 1958; pp 162–171, and references therein.
(19) Fukuda, A. *Phys. Rev. B* **1970**, *1*, 4161.
(20) Scacco, A.; Jacobs, P. W. M. *Lett. Nuovo Cimento Soc. Ital. Fiz.* **1982**, *33*, 535.
(21) Saltzberg, M. A. Ph.D. Thesis, University of Pennsylvania, 1988.
(22) Dunn, B., private communication.

Table II. Refined Atomic Positions and Occupancies for Sn(II) Ions in Anhydrous Sn(II)-β″-Alumina

atom	x	y	z	occupation, %
Sn(1)	0	0	0.1865 (0)	44.3 (4)[a]
Sn(1)′	0	0	−0.1865 (0)	35.9 (4)[a]

[a] One such site per conduction layer.

Table III. Refined Interatomic Distances in Anhydrous Sn(II)-β″-Alumina

contact	multiplicity	dist, Å
Sn(1)–O(3)	1	3.155 (2)
Sn(1)–O(4)	3	2.326 (1)
Sn(1)–O(5)	3	3.315 (1)

of 11-Å-thick layers involving aluminum ions octahedrally and tetrahedrally coordinated by oxygen ions. The aluminum ion, Al(2), at the center of these layers is approximately 33% substituted by Mg(II) ions. These so-called "spinel" blocks are separated from one another by the conduction layers and linked by Al–O–Al bonds perpendicular to the conduction layers and parallel to the *c* axis. This framework is well-known from studies of other isomorphs and was used as a starting point for the refinement of the structure of the Sn(II) isomorph.

The principal feature of interest in these structures is the arrangement of the mobile species in the conduction layer. In the case of the anhydrous compound, the only mobile species is Sn(II). But in the hydrated form, the conduction layers must also accommodate a roughly equal number of water molecules. The most common cation sites in the conduction layer are the tetrahedral Beevers–Ross (BR) sites and the roughly octahedral midoxygen (mO) sites. These sites are arranged in the form of a nearly two-dimensional honeycomb lattice. The BR sites are at the 3-fold nodes of the lattice (3*m* point symmetry), and the mO sites are centers of symmetry midway between them. The column oxygens (O5) occupy the site at the center of each hexagon of the honeycomb lattice. The arrangement of cations in the conduction layer and distortions in the oxide framework are influenced by the charge, size, and polarizability of the mobile cation.

The hexagonal lattice parameters for each sample were determined by least-squares refinement of 23 reflections in the 2ϑ range 29–39°. The unit cell parameters for the anhydrous sample are a = 5.6206 (5) Å and c = 34.311 (7) Å and a = 5.623 (1) Å and c = 34.191 (11) Å for the hydrated sample. The contraction of the c axis on water uptake is somewhat surprising and contrary to our findings for the Ba(II), Ca(II), and Pb(II) isomorphs.[23] This unusual behavior can be attributed to the observed redistribution of Sn(II) ions that occurs upon hydration.

In the first stages of refinement of the structure of the anhydrous compound, an observed Fourier synthesis was calculated by using a model including only the framework ions in their Na-β″-alumina positions. The result indicated that the Sn(II) ions were located at BR sites. In subsequent refinements, occupation, position, harmonic, and anharmonic thermal parameters were determined for the Sn(II) atoms. Positional and thermal parameters were also refined for the framework atoms (Tables II–V).

The refined concentration of Sn(II) ions was found to be 96% of the chemically determined value. All Sn(II) ions were found to occupy BR sites. Coulombic repulsion would be expected to exclude the occupation of adjacent BR sites by Sn(II) ions, since the number of sites exceeds the

Table IV. Refined Atomic Positions and Occupancies for Sn(II) Ions and Water Oxygens in Hydrated Sn(II)-β″-Alumina

atom	x	y	z	occupation
Sn(1)	0	0	0.1862 (1)	5.4 (1)[a]
Sn(1)′	0	0	−0.1862 (1)	15.2 (1)[a]
Sn(2)/OW(1)	−0.1143 (7)	$x/2$	0.1741 (1)	9.4 (2)/12.3[b]
Sn(2)′/OW(1)′	0.1143 (7)	$x/2$	−0.1741 (1)	9.4 (2)/12.3[b]

[a] One such site per conduction layer. [b] Three such sites per conduction layer.

Table V. Refined Interatomic Distances in Hydrated Sn(II)-β″-Alumina

contact	multiplicity	dist, Å
Sn(1)–O(4)	3	2.335 (2)
Sn(1)–O(3)	1	3.120 (3)
Sn(1)–O(5)	3	3.314 (1)
Sn(1)–Sn(2)′/OW(1)′	3	3.145 (2)
Sn(2)/OW(1)–O(4)	1	2.357 (4)
Sn(2)/OW(1)–O(5)	1	2.702 (4)
Sn(2)/OW(1)–Sn(2)′/OW(1)′	1	2.738 (2)
Sn(2)/OW(1)–O(3)	1	2.765 (4)
Sn(2)/OW(1)–O(4)	2	2.868 (8)
Sn(2)/OW(1)–Sn(2)′/OW(1)′	2	2.903 (2)

number of divalent ions by more than a factor of 2. This was investigated in the refinement process by allowing adjacent BR sites to refine independently in an otherwise centrosymmetric $R\bar{3}m$ space group. This technique was first used by Thomas et al. to study short-range order in Ba(II)-β″-alumina.[24] The refined occupation ratio of Sn(II) ions in adjacent BR sites was only 1.2:1, indicating only a small degree of short-range order in the Sn(II) arrangement. That Sn(II) ions appear to be distributed almost randomly among the BR sites would suggest that interactions between the mobile cations are relatively unimportant in determining the mobile ion arrangement in this isomorph.

The final observed Fourier synthesis of the electron distribution in and near the conduction plane of Sn(II)-β″-alumina is shown in Figure 8. Note that the cations have nearly spherical electron distributions well localized at BR sites. This contrasts markedly with electron density maps published for Pb(II)-β″-alumina,[6] which suggest Pb(II) ions spread out along the conduction pathways. The greater degree of localization can clearly be related to the observation that the ionic conductivity of Sn(II)-β″-alumina is lower than that of Pb(II)-β″-alumina. We now know, however, that the electron density distributions published for Pb(II)-β″-alumina were obtained from a sample that was almost certainly partially hydrated. A direct comparison of the two results is thus somewhat unsatisfactory.

There is also structural evidence that the interaction between Sn(II) ions and the framework is strong. The Sn(II) ions at BR sites have an asymmetric coordination: three equivalent Sn–O(4) bonds of length 2.326 (1) Å and an Sn–O(3) bond of 3.155 (2) Å. This elongated Sn–O(3) bond is the result of repulsion between the O(3) ion and the $5s^2$ lone pair of electrons that are presumably localized in this direction. This is a fine example of the lone-pair effect and must be regarded as the primary reason for the large *c* axis.

A vertical section through the observed Fourier synthesis (Figure 9) clearly shows the relationship between Sn(II) and framework ions. The relevant atomic positions and interatomic distances are shown schematically. It must

(23) Rohrer, G. S.; Thomas, J. O.; Farrington, G. C., manuscript in preparation.

(24) Thomas, J. O.; Alden, M.; McIntyre, G.; Farrington, G. C. *Acta Crystallogr.* **1984**, *B40*, 208.

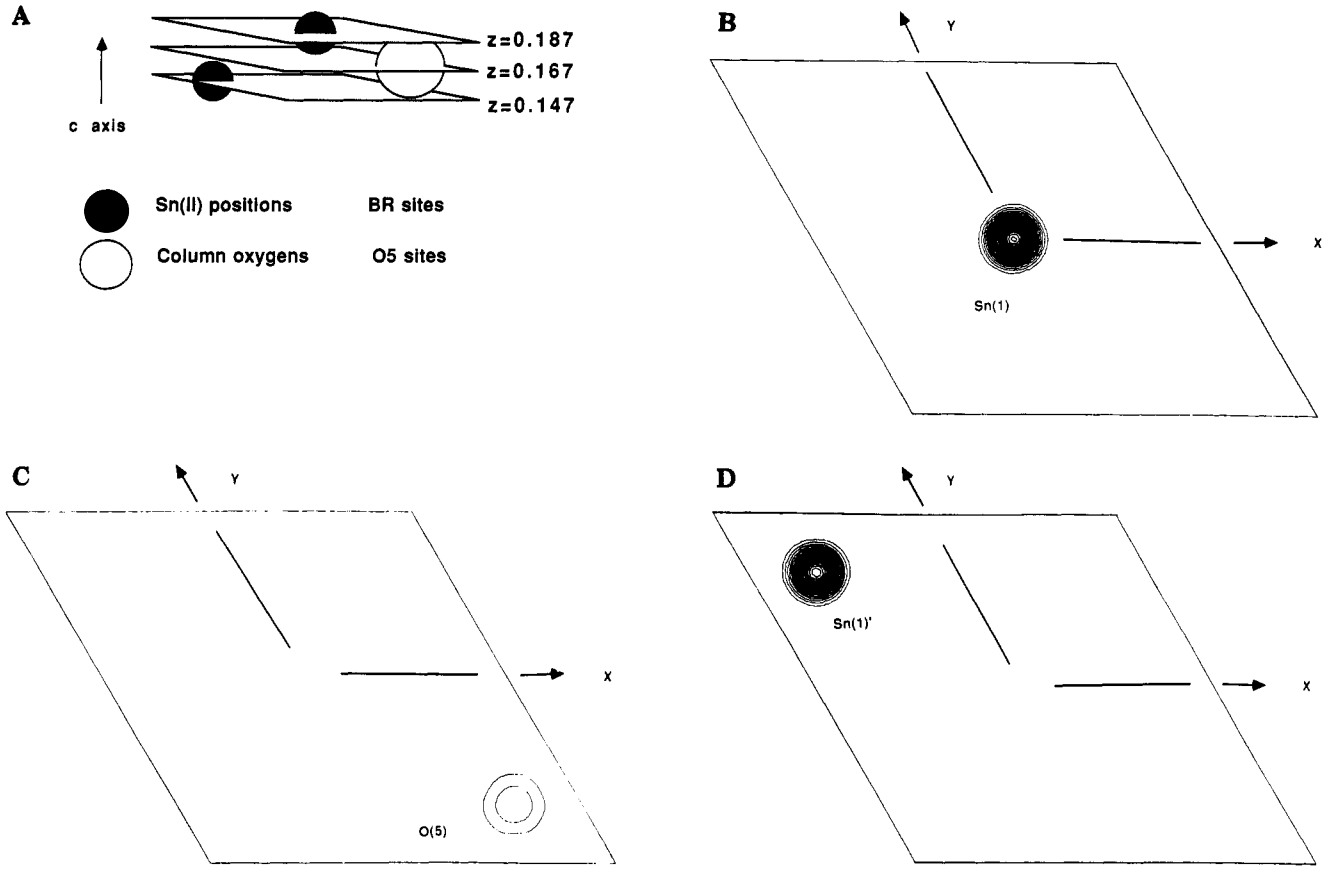

Figure 8. Conduction layer structure of Sn(II)-β″-alumina. (A) Three-dimensional schematic indicates the positions in the conduction layer from which the three slices of experimental data in B, C, and D were obtained. (B, C, and D) Three observed electron density maps calculated by using phases obtained from the refined structural model at z = 0.187 (B), 0.167 (C), and 0.147 (D). Levels are at 6.2 e/Å^3.

be remembered that the Sn(II) ion only partially occupies the BR sites, so the observed oxygen positions are actually the average for occupied and unoccupied Sn(II) sites. If it is assumed that the vacant sites are relatively symmetric, the actual local distortion around the Sn(II) ion must be even greater than that observed here.

It is interesting to compare structural data for the Sn(II) and Pb(II) isomorphs, since both are lone-pair ions. The lattice parameter for Pb(II)-β″-alumina is 33.96 Å, which is less than the Sn(II) isomorph. This is unexpected on the basis of traditional ionic radii values. However, such values are of little use for lone-pair ions bonded in solids. In fact, Shannon has concluded that the tendency for a Sn(II) ion to form distorted coordination polyhedra in solids makes the determination of its ionic radius relatively meaningless.[25] The difference in the bond distances is better understood by considering the interactions between the lone-pair ion and its ligands. Wells has noted that in compounds containing Sn(II) or Pb(II) with the same ligands of the same electronegativity, the lone-pair effect is always more pronounced in the Sn(II) compounds.[26] Indeed, more recent structural data indicate that the lone-pair distortion is relatively small in Pb(II)-β″-alumina.[27] The repulsion between the lone-pair and the O(3) oxygen would thus seem to cause the lengthening the Sn–O(3) bond, the unusually long c axis, and the cracking of many of the samples.

As previously noted, the ionic conductivity of Sn(II)-β″-alumina is much lower than that of Pb(II)-β″-alumina.

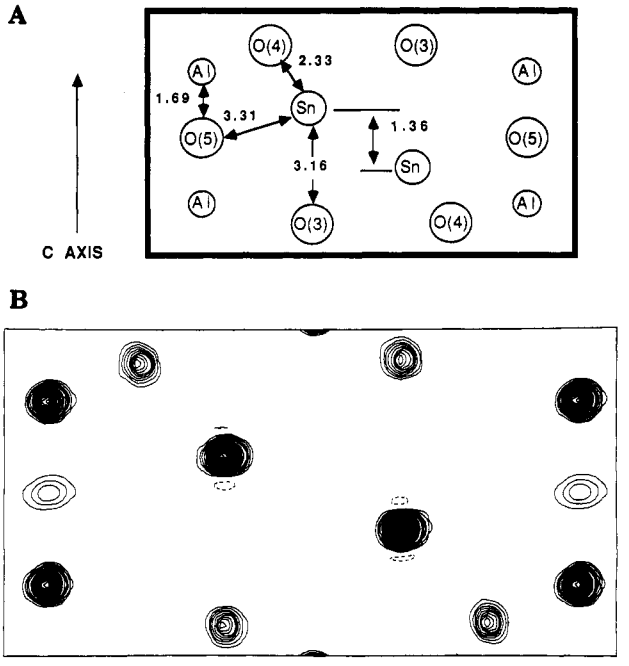

Figure 9. Vertical section through the conduction layer of anhydrous Sn(II)-β″-alumina. (A) Schematic diagram showing the atom types and interatomic distances. (B) Observed electron density maps calculated as in Figure 8. Al–O–Al bridging bonds are seen at each edge of the figure. Levels are at 4.5 e/Å^3.

It is tempting to speculate that the distortion of the coordination polyhedron around the Sn(II) ion lowers the potential energy of the cation and raises the activation barrier for conduction. This could account for the in-

(25) Shannon, R. D. *Acta Crystallogr.* **1976**, *A32*, 751.
(26) Wells, A. F. *Structural Inorganic Chemistry*, 5th ed.; Clarendon Press: Oxford, 1984; p 1182.
(27) Thomas, J. O., private communication.

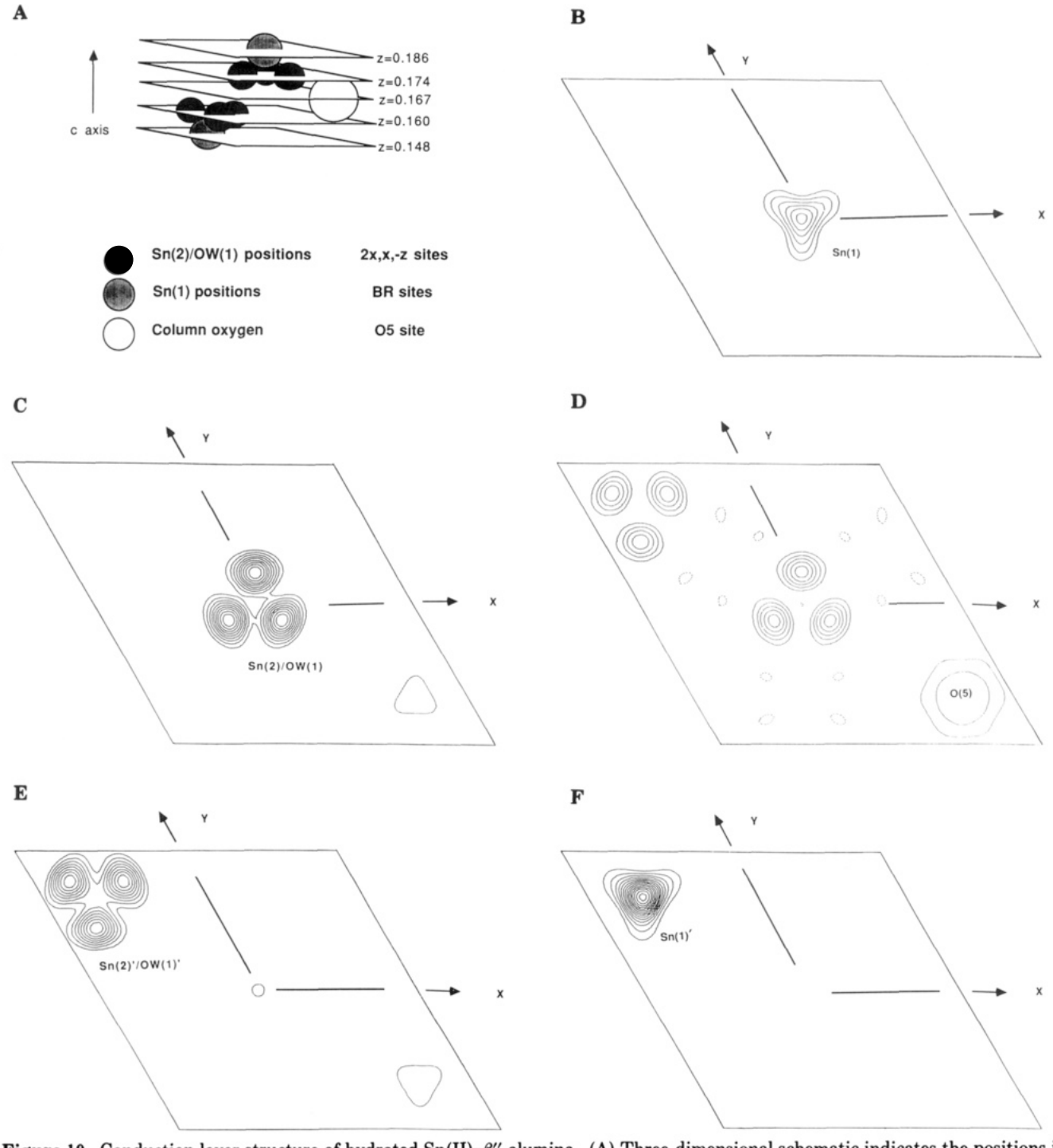

Figure 10. Conduction layer structure of hydrated Sn(II)–β''-alumina. (A) Three-dimensional schematic indicates the positions in the conduction layer from which the five slices of experimental data in B–F were obtained. (B–F) Five observed electron density maps calculated as in Figure 8. They represent five closely spaced planes along the c axis in the conduction layer at z = 0.186 (B), 0.174 (C), 0.167 (D), 0.160 (E), and 0.148 (F). Levels are at 3.0 e/Å^3.

creased activation energy for conduction observed in the Sn(II) isomorph. However, this cannot account for the low ionic conductivity of the other divalent isomorphs, such as Ca(II)– and Ba(II)–β''-alumina. These, like Pb(II)–β''-alumina, have more symmetrically coordinated mobile cations. A simplistic explanation for the anomalously high conductivity of the Pb(II) isomorph thus has eluded us once again.

For the hydrated compound, we again used an observed Fourier synthesis to determine the approximate positions of the Sn(II) ions and water molecules. The situation here was a little more complicated. Two positions contained electron density in the conduction layer: BR sites and ($2x$, x, $-z$) sites displaced away from the $3m$ axis along the conduction pathways. Refinement indicated that Sn(II) ions occupied both BR and ($2x$, x, $-z$) sites; the latter were also occupied by water oxygens. The overlapping Sn(II) and OW occupation could not be separated. The Sn(II) ions at BR sites were refined with both harmonic and anharmonic temperature factors. The water oxygen and Sn(II) ions at ($2x$, x, $-z$) sites were represented by an anisotropic thermal model. No extinction correction was needed.

The observed Fourier syntheses for five horizontal slices parallel to the conduction plane and a schematic diagram of the atom placement are shown in Figure 10. The best

refinement indicated that 73% of the Sn(II) atoms lie on $(2x, x, -z)$ sites together with the water (the water content was constrained to 0.74 molecules per formula unit). The remaining Sn(II) ions are on BR sites.

By comparison with the anhydrous structure, the hydrated structure is surprising. The arrangement of cations in the conduction layer is drastically altered by the intercalation of water: the favored site for the Sn(II) ion in the hydrated form becomes the asymmetric five-coordinate $(2x, x, -z)$ site. The shortest Sn–O interatomic distance becomes 2.738 (2) Å. This closest approach of a Sn(II) ion and a water molecule is 3.125 (2) Å. This configuration occurs when both the water molecule and Sn(II) ion occupy $(2x, x, -z)$ sites related by a center of symmetry. The water molecule thus interacts more strongly with oxygens in the spinel block than with the Sn(II) ions. A similar situation exists in hydrated Ca(II)–β''-alumina.[23] This structural information, together with the similarity of the binding energies for water in different isomorphs, suggests that the absorption of water by various β''-alumina compositions is principally the result of interaction between water molecules and the β''-alumina framework and is influenced less by cation type. A more complete description of the structure of the hydrated divalent β''-aluminas is provided elsewhere.[23]

The movement of 73% of the Sn(II) ions away from BR sites on water intercalation also explains the observed contraction of the c axis. Not only is the Sn(2)–O(3) bond shorter than in the anhydrous compound, it is also no longer parallel to the c axis. Structural rearrangements resulting from hydration may account for changes in other physical properties. Although the effect of hydration on the conductivity of the Sn(II) isomorph was not studied, the conductivity of Pb(II)–β''-alumina decreases as a result of hydration.[28] The same can be expected for the Sn(II) form.

Conclusions

Sn(II)–β''-alumina is a new luminescent solid electrolyte in the β''-alumina family of compounds. In this investigation we have characterized its synthesis, composition, structure, transport and optical properties, and most importantly, its reactivity with water. Sn(II)–β''-alumina hydrates readily, and the reaction affects both its structure and properties. We believe that Sn(II)–β''-alumina illustrates many of the complex phenomena that interact to determine the properties of the β''-alumina family of compounds. Understanding these materials requires a connected approach using many different characterization techniques. The results demonstrate some of the reasons these compounds are such intriguing and unusual inorganic materials.

Acknowledgment. This research was supported in Sweden by the National Science Research Council (NFR) and in the United States by the Office of Naval Research. Additional support by the National Science Foundation, Materials Research Laboratory Program, under Grant No. DMR-8519059 is gratefully acknowledged.

Registry No. $Sn_{0.83}Mg_{0.67}Al_{10.33}O_{17}·xH_2O$, 119356-42-2; $Sn_{0.83}Mo_{0.67}Al_{10.33}O_{17}$, 119356-36-4; $Na_{0.33}Mg_{0.67}Al_{10.33}O_{17}$, 127818-91-1.

Supplementary Material Available: Listings of interatomic distances and atomic positions (77 pages); listing of structure factor amplitudes (69 pages). Ordering information given on any current masthead page.

(28) Rohrer, G. S.; Farrington, G. C. *J. Solid State Chem.*, in press.

Bulk and Nanostructure Group II–VI Compounds from Molecular Organometallic Precursors

J. G. Brennan,† T. Siegrist, P. J. Carroll, S. M. Stuczynski, P. Reynders, L. E. Brus, and M. L. Steigerwald*

AT&T Bell Laboratories, Murray Hill, New Jersey 07974

Received February 8, 1990

We describe the preparation of the solid-state compounds ZnS, ZnSe, CdS, CdSe, CdTe, and HgTe from the corresponding $M(ER)_2$ compounds (M = Zn, Cd, Hg; E = S, Se, Te; R = *n*-butyl, phenyl) and/or phosphine complexes thereof. We have isolated members of two different families of phosphine complexes. In the first the bidentate phosphine 1,2-bis(diethylphosphino)ethane (DEPE) is coordinated to the $M(ER)_2$ nucleus in a 1:2 ratio, and a coordination polymer is formed. In the second the DEPE/$M(ER)_2$ ratio is unity, and a dimeric compound is formed. We show that pyrolysis of these compounds in the solid state yields the bulk solid-state compound and that pyrolysis in solution yields the same solid-state compound, but in the form of nanometer-sized particles. Nanoclusters of HgTe are similarly formed by solution-phase photolysis of $Hg(TeBu)_2$.

Introduction

Precursors to group II–VI materials have been the focus of recent synthesis efforts. This work has been motivated by the desire to prepare group II–VI materials in a variety of physical forms, notably as quantum wells or quantum dots. A number of workers have shown that $M(ER)_2$ complexes (M = Zn, Cd, Hg; E = S, Se, Te; R = organic moiety) can be converted to the related solid-state compounds,[1] but unfortunately these molecular precursors are

† Current address: Department of Chemistry, Rutgers University, P.O. Box 939, Piscataway, NJ 08855.

* Author to whom correspondence should be addressed.

(1) (a) Kern, R. J. *J. Am. Chem. Soc.* **1953**, *75*, 1865. (b) Peach, M. E. *J. Inorg. Nucl. Chem.* **1973**, *35*, 1046. (c) Peach, M. E. *J. Inorg. Nucl. Chem.* **1979**, *41*(9), 1390. (d) Osakada, K.; Yamamoto, T. *J. Chem. Soc., Chem. Commun.* **1987**, 1117. (e) Steigerwald, M. L.; Sprinkle, C. R. *J. Am. Chem. Soc.* **1987**, *109*, 7200. (f) Brennan, J. G.; Siegrist, T.; Carroll, P. J.; Stuczynski, S. M.; Brus, L. E.; Steigerwald, M. L. *J. Am. Chem. Soc.* **1989**, *111*, 4141.

0897-4756/90/2802-0403$02.50/0